Tenth International Conference on Computational Fluid Dynamics (ICCFD10), Barcelona,Spain, July 9-13, 2018

ICCFD10-2018-245

Unsteady Impulsive Jet Applied to a Stalled Airfoil

T. Kim*, J. Kim* S. Kim* J. Lee* and S. Jee*
Corresponding author: sjee@gist.ac.kr

* Gwangju Institute of Science and Technology, South Korea.

Abstract: The ability to control a separating boundary layer can improve aerodynamic performance of a lifting body. It is natural to investigate flow control methods for a stalled airfoil because of straightforward analysis of the control impact on aerodynamic forces. In this study, unsteady impulsive jet is used for the separation control. The impulsive jet is generated from a combustion-powered actuator located on the suction side near the leading edge. The performance of the impulsive jet is numerically evaluated for static stall conditions. The current flow condition of $Mach$=0.3 and Re=2.6 million is relevant to the retreating blade stall of a rotorcraft main rotor. The VR-12 airfoil, an advanced rotorcraft blade airfoil, is simulated with the compressible flow solver, SU2. To model impulsive jet, a time-dependent inflow boundary condition is implemented in the solver. Unsteady Reynolds-averaged Navier-Stokes computations with the Spalart-Allmaras model is used for turbulence simulation. Current computational results show good agreement with the experimental results. Lift enhancement are observed at high angles of attack with COMPACT.

Keywords: Active Flow Control, Combustion-Powered Actuation (COMPACT), Stalled Airfoil, Computational Fluid Dynamics.

1 Introduction

Dynamic stall occurs on the retreating side of a helicopter main rotor, limiting the rotor performance in high-speed forward flight conditions. Adverse effects of the retreating blade stall can be mitigated by controlling the separated boundary layer.

Various control methods have been studied and applied for the reattachment of separated flow [1]. Control surfaces such as leading-edge slats [2, 3, 4], miniature trailing-edge effectors [5, 6], and vortex generators [7] augment the aerodynamic lift, suppressing the flow separation. These control-surface methods, however, cause drag penalties at high speeds.

Fluidic actuation techniques have been developed to achieve improved aerodynamic performances with minimized drag penalties. In this study, unsteady impulsive jet is used for the stall suppression. The unsteady jet is generated from a small combustion chamber [8]. Combustion process creates a significant pressure rise in the chamber, which results in high-velocity jet through an opening to the external flow. The duration of the impulsive jet is brief, typically around 1msec. The jet velocity is near sonic because the internal flow in the actuator slot is chocked. This fluidic actuation is often referred to combustion-powered actuation (COMPACT) in the literature. COMPACT does not require a moving part, which helps to initiate combustion with a high frequency up to 100-200Hz [9].

2 Computational Method

The VR-12 airfoil, an advanced rotorcraft airfoil, is simulated with the unsteady impulsive jet (see Fig. 1). The clean airfoil with the 5% trailing-edge tab was numerically investigated by the authors in the previous study [10]. Following the wind tunnel test[9], the actuator is located on the suction side at x/c=0.1, where c is the chord length. The structure constraint allowed the slot angle to be 22 degrees as the minimum [9, 11]. The actuator slot is designed such that the jet is tangentially ejected to the suction side of the airfoil.

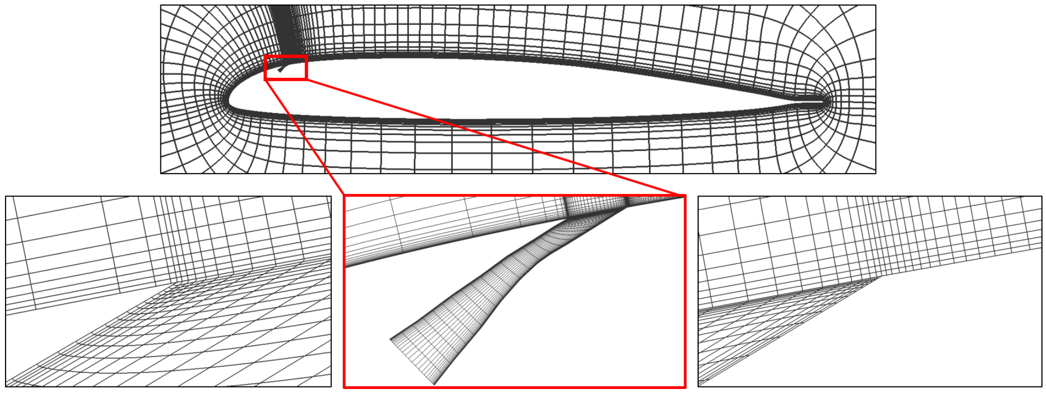

Figure 1: Grid around the VR-12 airfoil and the actuator slot. Every 4th grid point is shown.

The number of the current gird points is 761x145 for the external flow field around the airfoil and 145x129 for the actuator slot. Free-stream is located at $50c$ away from the airfoil.

The conservative form of the compressible Navier-Stokes equation is numerically solved using the Stanford University Unstructured (SU2) flow solver [12]. The second-order dual-time stepping method is used for the temporal discretization [13]. The Courant-Friedrich-Lewy (CFL) number for the internal iteration is 4, and the number of the subiterations are 100 which is sufficient for the convergence of the subiteration. The second-order Roe scheme is used for the Euler fluxes [14]. Unsteady Reynolds-averaged Navier-Stokes (URANS) computation is conducted with the Spalart-Allmaras (SA) model [15].

The following rotor-relevant flow condition is used here: $Mach$=0.3 and Re=2.6million. A time-dependent inflow boundary condition is applied to model the impulsive actuation shown in Fig. (2). The actuator boundary condition switches from an inflow to a wall condition. When the impulsive jet is generated, the inflow boundary condition is applied on the actuator boundary with the total pressure and the total temperature. The inflow jet is ejected normal to the actuator boundary. After the duration of the impulsive jet, the no-slip wall condition is applied on the actuator. The measured pressure in the COMPACT actuator P_{act} [9] is used in the current simulation. The time-dependent pressure is given by Eq.(1).

$$P_r(t) = 0.5\left[cos\left(2\pi\frac{t-t_0}{T_{act,pulse}} - \pi\right) + 1.0\right](P_{r,peak} - 1.0) + 1.0 \tag{1}$$

where the pressure ratio is defined as $P_r = P_{act}/P_0$, P_0 is the pressure outside the actuator, $P_{r,peak}$ is the peak pressure ratio, $T_{act,pulse}$ is the pulse frequency. The pulse frequency is $T_{act,pulse}$=0.7msec, the peak pressure ratio value is $P_{r,peak}$=2.27, and the actuation frequency is f_{act}=110Hz yielding the non-dimensional actuation frequency $F^+ = f_{act}(c/U_\infty)$=0.4. The number of time steps per the jet duration is 35.

3 Computational Results

3.1 Static Airfoil Simulation

The static VR-12 airfoil without actuation is simulated at various angles of attack. Current computations are compared with the previous experimental and computational studies of [9, 11] (see Fig. 3). The experiments were are conducted at the NASA Glenn Icing Research Tunnel [9]. The chord length of the wing model is c=0.381 meter. The wing model in the test covers the test section with the spanwise length of 0.91 meter.

The aerodynamic lift, drag, and moment of the VR-12 airfoil without the actuation are reasonably well matched with the experimental data. The maximum lift and the static stall angle are well predicted. Beyond the static stall, both the CFL3D simulation of Jee et al [11] and the current simulation yield a rather smooth drop, compared to the experiment. In the linear-slope region, a constant shift in the lift is observed. This can be related to the flow angularity variation in the test facility, $\Delta\alpha = \pm 0.5°$ [6, 11]. Good agreement to

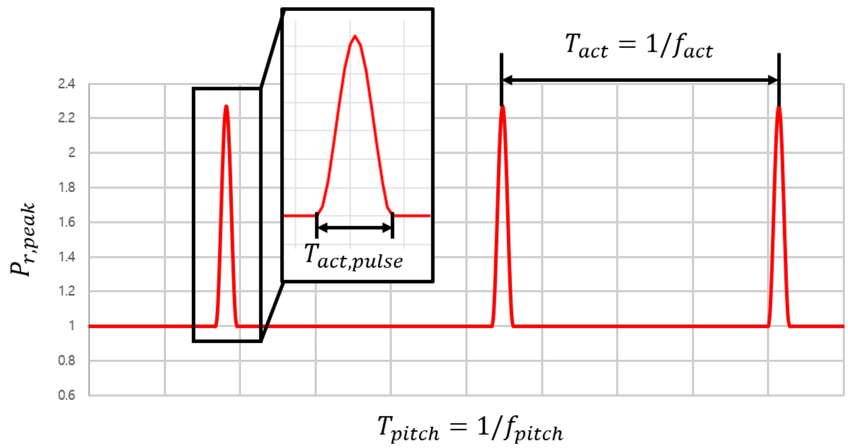

Figure 2: Overview of parameters for the impulsive jet and the sinusoidal function of the actuation.

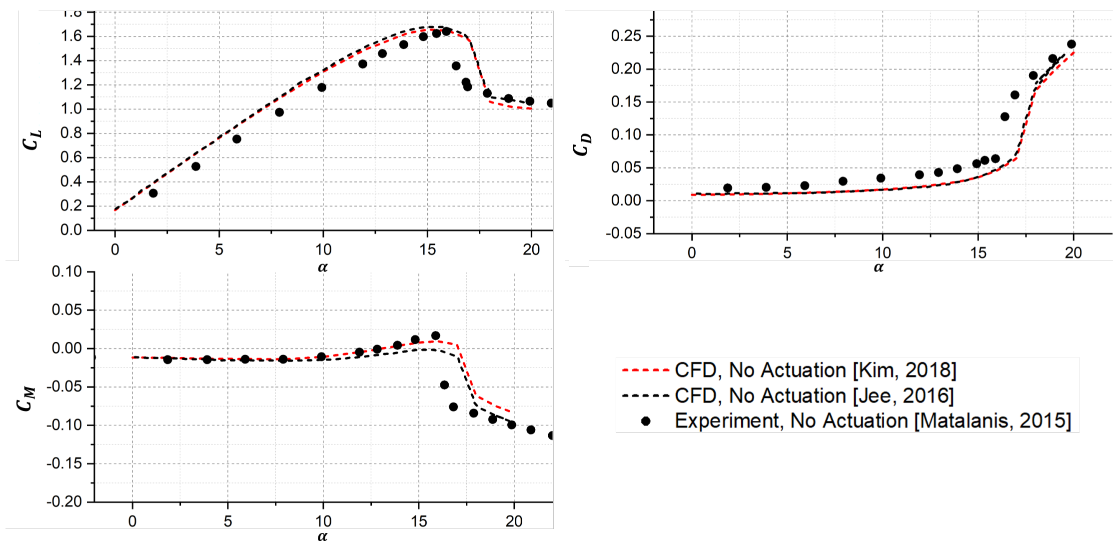

Figure 3: Aerodynamic forces of the VR-12 airfoil without actuation, $Mach$=0.3, and Re=2.6M

the experimental drag and moment is achieved in the current computation.

Pressure profiles are compared with the experimental data, as shown in Fig. 4. Overall, a good agreement is achieved in the current computation. Slightly higher suction peaks are observed in the simulation before the static stall. For higher angles $\alpha \geq 18°$, the separated region is clearly noticeable in the profile with excellent agreement to the test data.

The modified VR-12 airfoil with COMPACT is simulated for actuation cases, and compared against the previous studies [9, 11]. The current computation is able to reproduce the lift augment after the static stall. More comparison on the other aerodynamic coefficients and the pressure profile will be pursued.

3.2 Pitching Airfoil Simulation

The pitching airfoil with COMPACT is simulated. The actuation frequency F^{+}=0.4 is used with the reduced frequency k=0.07, where k is $k = \pi f_{pitch} c/U_{\infty}$. The pitching motion is prescribed as $\alpha = \alpha_0 + \alpha_1 sin(2kt/t_c)$. For the current simulation, α_0=10 and α_1=10. The pitch convergence is achived after five cycles. Hysteresis loops of the aerodynamic forces are shown in Fig. 6. A significant lift enhancement is observed in the down-stroke region from both the experiment and the computation. The negative moment peak is slightly

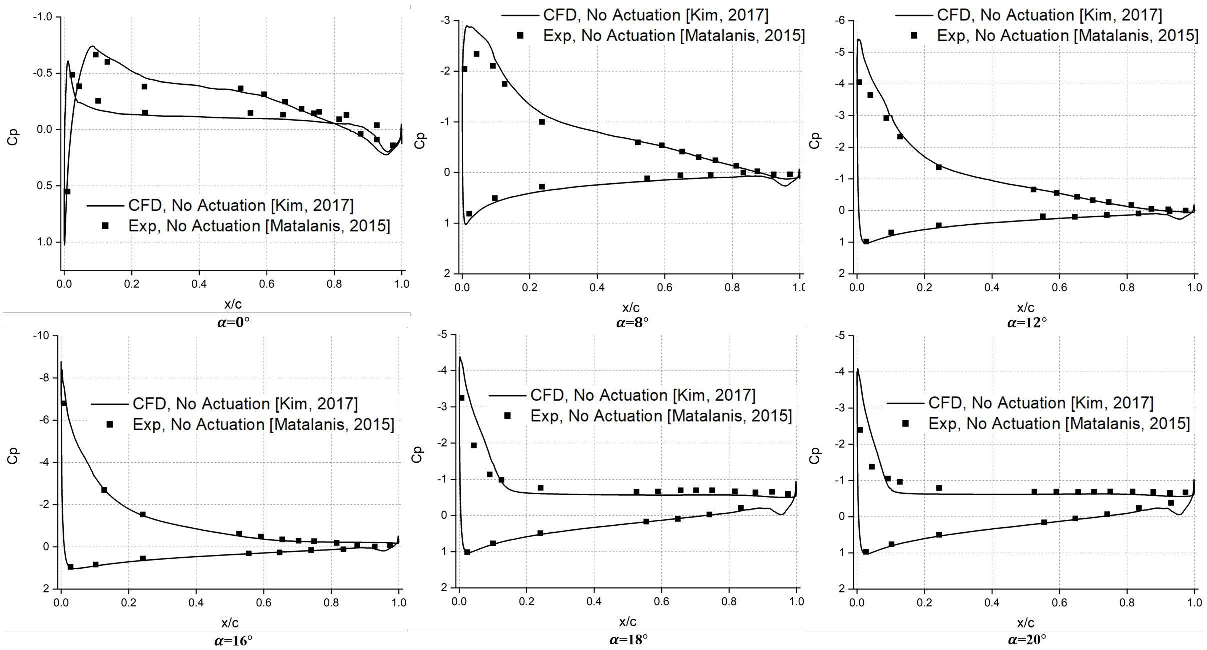

Figure 4: Pressure profiles of the VR-12 airfoil without actuation, $Mach$=0.3, Re=2.6M.

reduced in the computation.

4 Conclusion

Impulsive jet is numerically investigated with the VR-12 airfoil with the rotor-relevant flow condition, $Mach$=0.3, Re=2.6 million and k=0.07. COMPACT is located at x/c = 0.1 on the suction side of the VR-12 airfoil, generating the impulsive jet tangentially to the external boundary layer.

For the non-actuated case, the aerodynamic forces and the pressure profile are compared well with the previous experimental studies. The brief, impulsive jet is numerically modelled with the time-dependent boundary condition applied at the actuator. A significant lift enhancement is observed beyond the static stall angle, as observed in the wind tunnel test. For the pitching airfoil with the actuation, the lift in the down-stroke region is well recovered. The negative moment peak is slightly reduced in the current simulation.

Current computations are conducted in two dimensions. Experimental data indicate three dimensional aspects with COMPACT due to the finite span of the actuated region on the VR-12 wing. Three dimensional computations, incorporating major 3D effects in the test would be required.

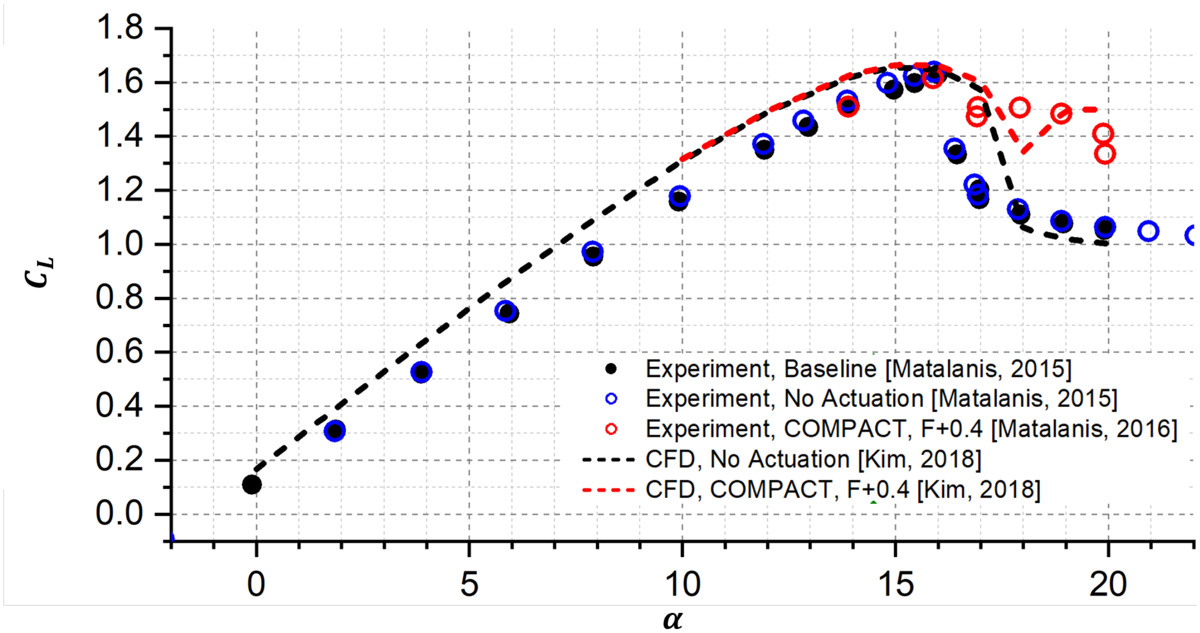

Figure 5: Aerodynamic lift of the VR-12 airfoil with actuation, $Mach$=0.3, Re=2.6M, F^+=0.4.

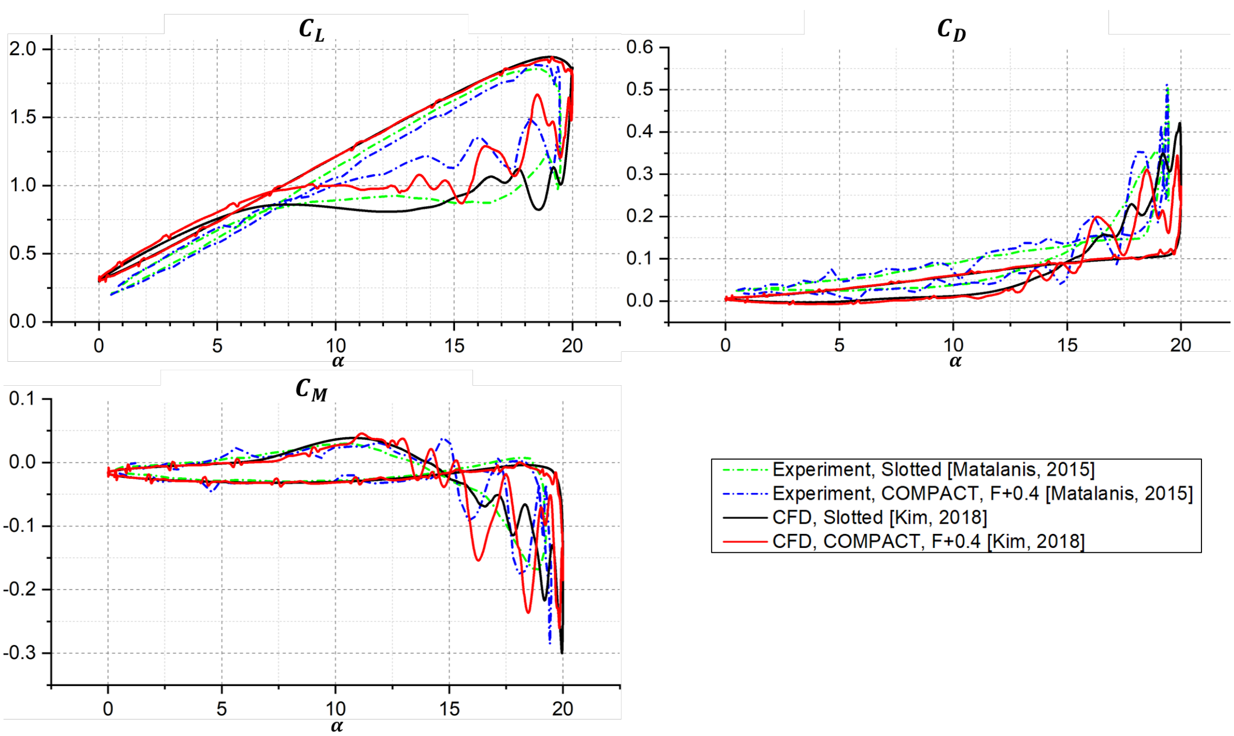

Figure 6: Aerodynamic forces and moment of the pitching VR-12 airfoil $Mach$=0.3, Re=2.6M, k=0.07, and F^+=0.4.

Acknowledgement

This work was supported by the National Research Foundation of Korea(NRF) grant funded by the Korea government(MSIT) (No. NRF-2017R1C1B5018300). This work was supported by the National Institute of Supercomputing and Network/Korea Institute of Science and Technology Information with supercomputing resources including technical support (Project No. KSC-2016-S1-0037). This work was supported by Global University Project(GUP) grant funded by the GIST in 2018.

References

[1] M. Gad-el Hak. *Flow Control: Passive, Active, and Reactive Flow Management.* Cambridge University Press, 2000.

[2] K. W. McAlister and C. Tung. Suppression of Dynamic Stall with a Leading-Edge Slat on VR-7 Airfoil. 1993.

[3] P. F. Lorber, A. Bagai, and B. E. Wake. Design and Evaluation of Slatted Airfoils for Improved Rotor Performance. Technical Report 1, 2006.

[4] A. Mishra, S. Ananthan, J. D. Baeder, D. G. Opoku, B. E. Wake, and R. S. Lin. Coupled CFD/CSD Prediction of the Effects of Leading Edge Slat on Rotor Performance. Technical report, 2009.

[5] M. P. Kinzel, M. D. Maughmer, and G. A. Lesieutre. Miniature Trailing-Edge Effectors for Rotorcraft Performance Enhancement. *Journal of the American Helicopter Society*, 52(2):146–158, 2007.

[6] C. G. Matalanis, B. E. Wake, D. Opoku, B. Min, N. Yeshala, and L. Sankar. Aerodynamic Evaluation of Miniature Trailing-Edge Effectors for Active Rotor Control. *Journal of Aircraft*, 48(3):995–1004, 2011.

[7] A. L. Pape, M. Costes, G. Joubert, F. David, and J. Deluc. Dynamic Stall Control Using Deployable Leading-Edge Vortex Generators. *AIAA Journal*, 50(10):2135–2145, 2012.

[8] T. Crittenden, A. Glezer, R. Funk, and D. Parekh. Combustion-Driven Jet Actuators for Flow Control. 15th AIAA Computational Fluid Dynamics Conference, 2001.

[9] C. G. Matalanis, B. Min, P. O. Bowles, S. Jee, B. E. Wake, T. M. Crittenden, G. Woo, and A. Glezer. Combustion-Powered Actuation for Dynamic-Stall Suppression: High-Mach Simulations and Low-Mach Experiments. *AIAA Journal*, 53(8):2151–2163, 2015.

[10] T. Kim, M. Kim, J. Kim, and S. Jee. Computations of an Advanced Rotorcraft Airfoil Using SU2. The Korean Society of Mechanical Engineers Forum 2017, 2017.

[11] S. Jee, C. Matalanis, B. Min, P. Bowles, B. Wake, T. Crittenden, and A. Glezer. Computations of Combustion-Powered Actuation for Dynamic Stall Suppression. 72nd American Helicopter Society (AHS) Annual Forum, 2016.

[12] Francisco Palacios, J. Alonso, K. Duraisamy, M. Colonno, J. Hicken, A. Aranake, A. Campos, S. Copeland, T. Economon, A. Lonkar, T. Lukaczyk, and T. Taylor. Stanford University Unstructured (SU2): An Open-Source Integrated Computational Environment for Multi-Physics Simulation and Design. *51st AIAA Aerospace Sciences Meeting including the New Horizons Forum and Aerospace Exposition*, page 287, 2013.

[13] A. Jameson. Time Dependent Calculations Using Multigrid, with Applications to Unsteady Flows Past Airfoils and Wings. page 1596, 1991.

[14] P. L. Roe. Approximate Riemann Solvers, Parameter Vectors, and Difference Schemes. *Journal of computational physics*, 43(2):357–372, 1981.

[15] P. R. Spalart and S. R. Allmaras. A One-Equation Turbulence Model for Aerodynamic Flows. Technical report, 1992.